A Unified Passivity Based Control Framework for Position, Torque and Impedance Control of Flexible Joint Robots

Alin Albu-Schäffer, Christian Ott, and Gerd Hirzinger

Institute of Robotics and Mechatronics, German Aerospace Center (DLR)
Alin.Albu-Schaeffer@dlr.de, Christian.Ott@dlr.de, Gerd.Hirzinger@dlr.de

Summary. In this paper we describe a general passivity based framework for the control of flexible joint robots. Herein the recent DLR results on torque-, position-, as well as impedance control of flexible joint robots are summarized, and the relations between the individual contributions are highlighted. It is shown that an inner torque feedback loop can be incorporated into a passivity based analysis by interpreting torque feedback in terms of shaping of the motor inertia. This result, which implicitly was already included in our earlier works on torque- and position control, can also be seized for the design of impedance controllers. For impedance control, furthermore, potential shaping is of special interest. It is shown how, based only on the motor angles, a potential function can be designed which simultaneously incorporates gravity compensation and a desired Cartesian stiffness relation for the link angles.
All the presented controllers were experimentally evaluated on the DLR light-weight robots and proved their performance and robustness with respect to uncertain model parameters. Herein, an impact experiment is presented briefly, and an overview of several applications is given in which the controllers have been applied.

1 Introduction

The currently growing research interest in application fields such as service robotics, health care, space robotics, or force feedback systems has led to an increasing demand for light robot arms with a load to weight ratio comparable to that of human arms. These manipulators should be able to perform compliant manipulation in contact with an unknown environment and guarantee the safety of humans interacting with them. A major problem which is specific to the implementation of light-weight robot concepts is the inherent flexibility introduced into the robot joints. Consequently, the success in the above mentioned robotics fields is strongly dependent on the design and implementation of adequate control strategies which can:

- compensate for the weakly damped elasticity in the robot joints in order to achieve high performance motion control,
- provide a desired Cartesian compliant behaviour of the manipulator,
- enable robust and fast manipulation in contact with unknown, passive environments,
- provide safety and dependability in interaction with humans.

It is commonly recognized that these control goals require measurement capabilities which clearly exceed the classical position sensing of industrial robots. The solution chosen in the case of the DLR light-weight robots (Fig. 1) was to provide the joints with torque sensors in addition to motor position sensors [12]. Additionally, a 6 dof force-torque sensor was mounted on the robot wrist. The position control problem for flexible joint robots was extensively treated

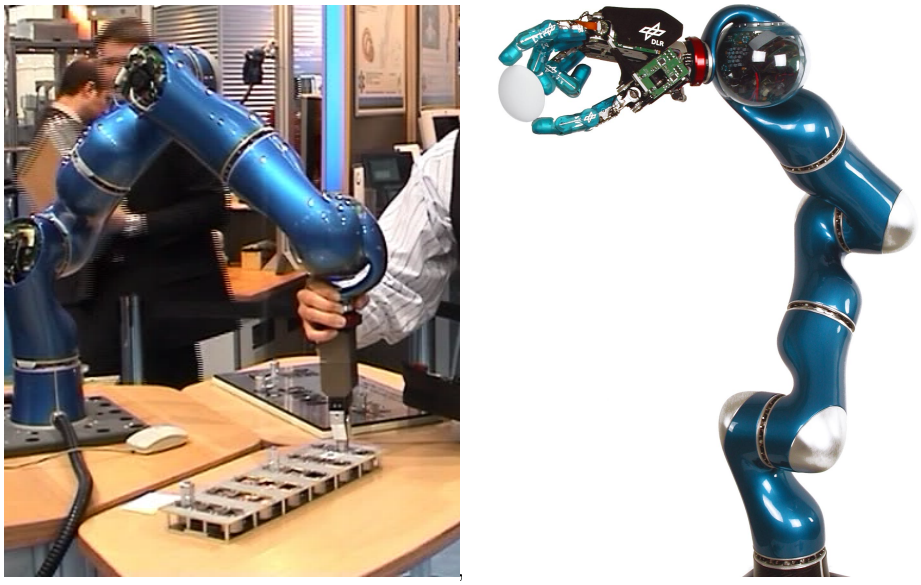

Fig. 1. The DLR light-weight robot III

in the robot control literature [17, 19, 8, 10, 14]. However, the problem of compliant motion control for interaction with unknown environments and with humans is addressed only recently under consideration of robot flexibility. The relevance of the topics becomes clear by looking at latest hardware developments, where elasticity is deliberately introduced into the joints in order to increase the interaction performance and the safety of robots [18, 21, 7]. Due to the fact that the model structure is slightly more complex than for rigid robots, there was still a gap between theoretical solutions (which often require very accurate models and the measurement or estimation of high derivatives of the joint position) and the practical solutions commonly chosen, which are

not always based on firm theoretical background.
In this paper we give an overview of the controller structures for the DLR robots, sketch the passivity based theoretical framework on which the actual controllers are based, go into some detail with the Cartesian impedance controller, and shortly describe some typical applications.

2 Controller overview

The first stage in the controller development was a joint state feedback controller with compensation of gravity and friction [2, 1]. The state vector contains the motor positions, the joint torques, as well as their first derivatives. By an appropriate parameterization of the feedback gains, the controller structure can be used to implement position, torque or impedance control. Based on this

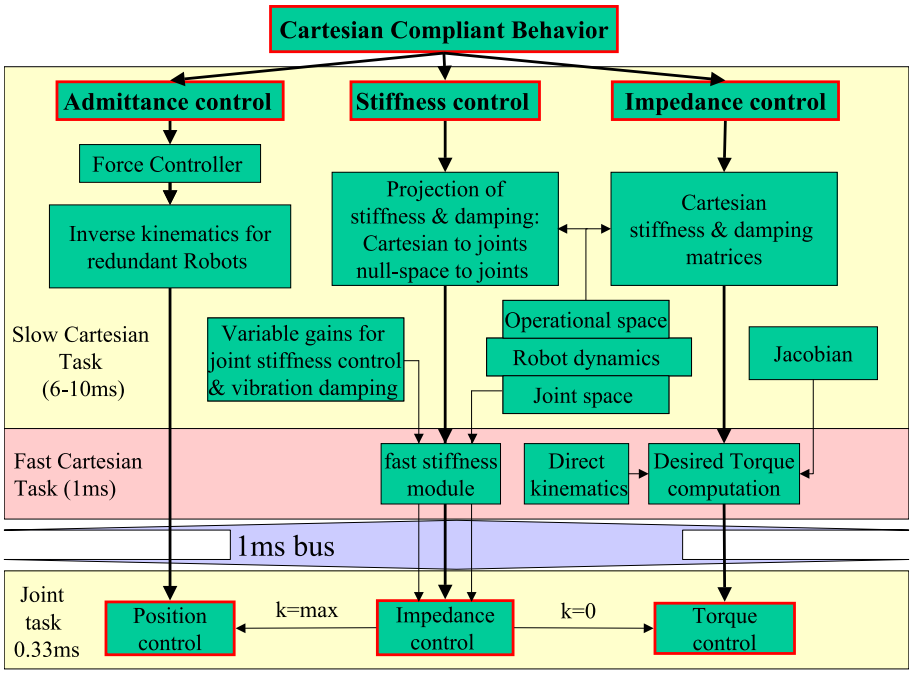

Fig. 2. Controller architecture for DLR's light-weight robots

joint control structure, three different strategies for implementing Cartesian compliant motion have been realized: admittance control, which accesses the joint position interface through the inverse kinematics; Cartesian impedance control, which is based on the joint torque interface; and Cartesian stiffness control, which accesses the joint impedance controller (Fig.2).

The latest developments focused on strategies for impedance control based on a passivity approach under consideration of the joint flexibilities [16, 5, 4]. A physical interpretation of the joint torque feedback loop has been given as the shaping of the motor inertia, while the implementation of the desired stiffness can be regarded as shaping of potential energy. Therefore, the Cartesian impedance controller can be designed and analyzed within a passivity based framework in the same manner as the previously mentioned state feedback controller.
The following model structure based on [17] is assumed for the flexible joint robot:

$$\boldsymbol{M}(\boldsymbol{q})\ddot{\boldsymbol{q}} + \boldsymbol{C}(\boldsymbol{q},\dot{\boldsymbol{q}})\dot{\boldsymbol{q}} + \boldsymbol{g}(\boldsymbol{q}) = \boldsymbol{\tau} + \boldsymbol{D}\boldsymbol{K}^{-1}\dot{\boldsymbol{\tau}} + \boldsymbol{\tau}_{\text{ext}} \tag{1}$$

$$\boldsymbol{B}\ddot{\boldsymbol{\theta}} + \boldsymbol{\tau} + \boldsymbol{D}\boldsymbol{K}^{-1}\dot{\boldsymbol{\tau}} = \boldsymbol{\tau}_m \tag{2}$$

$$\boldsymbol{\tau} = \boldsymbol{K}(\boldsymbol{\theta} - \boldsymbol{q}) \tag{3}$$

The vectors $\boldsymbol{q} \in \Re^n$ and $\boldsymbol{\theta} \in \Re^n$ contain the link and motor side positions respectively. $\boldsymbol{M}(\boldsymbol{q}) \in \Re^{n\times n}$, $\boldsymbol{C}(\boldsymbol{q},\dot{\boldsymbol{q}})\dot{\boldsymbol{q}}$, and $\boldsymbol{g}(\boldsymbol{q}) \in \Re^n$ are the components of the rigid body dynamics: inertia matrix, centripetal and Coriolis vector, and gravity vector. The vector $\boldsymbol{\tau} \in \Re^n$ represents the joint torques, $\boldsymbol{\tau}_{\text{ext}} \in \Re^n$ the external torques acting on the robot, and $\boldsymbol{\tau}_m \in \Re^n$ the motor torques. $\boldsymbol{K} = \text{diag}(K_i) \in \Re^{n\times n}$ and $\boldsymbol{B} = \text{diag}(B_i) \in \Re^{n\times n}$ are the diagonal, positive definite joint stiffness, and motor inertia matrices, respectively, and $\boldsymbol{D} = \text{diag}(D_i) \in \Re^{n\times n}$ is the diagonal positive semi-definite joint damping matrix.

3 Passivity based framework for torque, position and impedance control

In the following we summarize the approaches finally adopted for the DLR robots for torque, position, and impedance control and give a unified, passivity based view to these problems. Of course, the control literature for flexible joint robots contains various different other possible approaches to the problem. The best performance is theoretically given by decoupling based approaches, which provide a partially or even fully linearized closed loop system and ensure asymptotic stability also for the tracking case [17, 8, 14, 11, 15]. These controllers, however, require as a state vector the link side positions up to their third derivative and a very accurate robot model. For the DLR robots these approaches resulted in only moderate performance and robustness. The situation with back-stepping based controllers is similar to that of decoupling based approaches. On the other hand, singular perturbation based controllers are easy to implement, but their performance is theoretically and practically limited to the case of relatively high joint stiffness.
For the DLR light-weight robots, we preferred the passivity based approach

described below, because it is based only on the available motor position and joint torque signals, as well as their first order derivatives and it provides a high degree of robustness to unmodeled robot dynamics and in contact with unknown environments. It provides a framework which is both theoretically sound and also practically feasible, as demonstrated by the various applications realized so far using these controllers.

3.1 Passivity based joint position control

The starting point in the control development was a joint state feedback controller given by

$$\begin{aligned}\boldsymbol{\tau}_m = &-\boldsymbol{K}_P\tilde{\boldsymbol{\theta}} - \boldsymbol{K}_D\dot{\boldsymbol{\theta}} \\ &+\boldsymbol{K}_T(\boldsymbol{g}(\boldsymbol{q}_s) - \boldsymbol{\tau}) - \boldsymbol{K}_S\dot{\boldsymbol{\tau}} + \boldsymbol{g}(\boldsymbol{q}_s)\end{aligned} \tag{4}$$

with $\boldsymbol{K}_P$, $\boldsymbol{K}_D$, $\boldsymbol{K}_T$, and $\boldsymbol{K}_S$ being positive definite diagonal matrices and with a gravity compensation $\boldsymbol{g}(\boldsymbol{q}_s)$ based on the desired position. This constitutes an extension of the PD controllers from [19] to a full state feedback. Under some conditions related to the minimal eigenvalues of $\boldsymbol{K}_P$ and $\boldsymbol{K}_D$ [2, 1], the controller together with the motor side dynamics (2) can be shown to provide a passive subsystem, what in turn leads to passivity of the entire closed loop system[1], as sketched in Fig.3. In [1] it was exemplified that by ad-

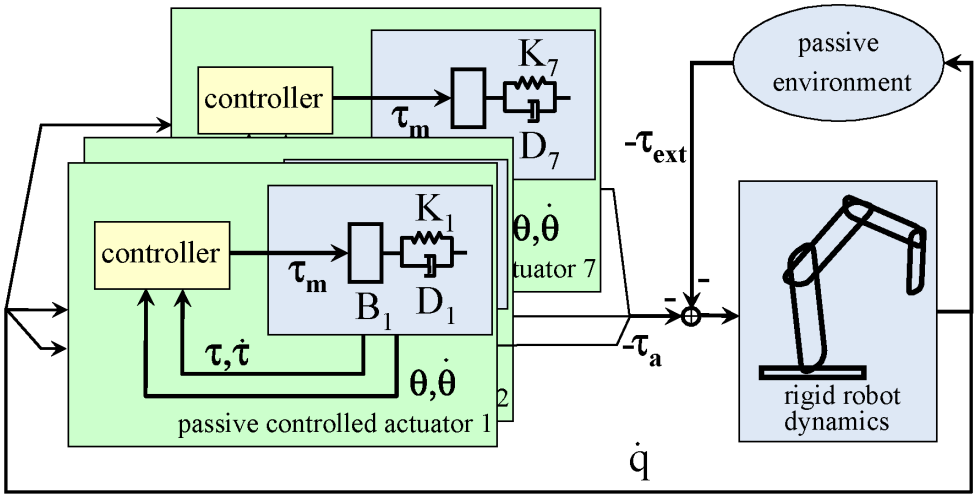

Fig. 3. Representation of the robot as a connection of passive blocks

[1] Passivity is given in this case, e.g. with respect to the variables $\{\boldsymbol{\tau}_a, \dot{\boldsymbol{q}}\}$, with $\boldsymbol{\tau}_a = \boldsymbol{\tau} + \boldsymbol{D}\boldsymbol{K}^{-1}\dot{\boldsymbol{\tau}}$.

equately designing the controller gains $\boldsymbol{K}_P$, $\boldsymbol{K}_D$, $\boldsymbol{K}_T$, and $\boldsymbol{K}_S$, the structure can be used to implement a torque, position or impedance controller on joint level.

3.2 Joint torque control: shaping the actuator kinetic energy

In order to be able to generalize the joint level approach also to Cartesian coordinates, the idea of interpreting the joint torque feedback as the shaping of the motor inertia plays a central role [16]. It enables to directly use the torque feedback within the passivity framework and conceptually divides the controller design into two steps, one related to the torque feedback and the other to the position feedback. However, in contrast to singular perturbation approaches, the analysis does not require the two loops to have different time scales, which would imply very high bandwidth for the torque controller.
Consider a torque feedback of the form

$$\boldsymbol{\tau}_m = \boldsymbol{B}\boldsymbol{B}_\theta^{-1}\boldsymbol{u} + (\boldsymbol{I} - \boldsymbol{B}\boldsymbol{B}_\theta^{-1})(\boldsymbol{\tau} + \boldsymbol{D}\boldsymbol{K}^{-1}\dot{\boldsymbol{\tau}}). \tag{5}$$

Herein $\boldsymbol{u} \in \Re^n$ is an intermediate control input. In [5] a more general form of this torque controller was presented, in which the feedback gain of $\dot{\boldsymbol{\tau}}$ is an additional independent design parameter, giving the possibility to optimize the performance and the vibration damping effect of the controller. Due to lack of space, the presentation will be restricted here to the simpler case given by (5). The torque controller leads together with (2) to

$$\boldsymbol{B}_\theta\ddot{\boldsymbol{\theta}} + \boldsymbol{\tau} + \boldsymbol{D}\boldsymbol{K}^{-1}\dot{\boldsymbol{\tau}} = \boldsymbol{u} \tag{6}$$

Comparing (2) with (6) it is clear that the effect of the torque controller is that of changing the motor inertia to $\boldsymbol{B}_\theta$ for the new subsystem with input $\boldsymbol{u}$.

3.3 Motor position based feedback: shaping the potential energy

First notice that for the joint control case, a controller of the form

$$\boldsymbol{u} = -\boldsymbol{K}_\theta\tilde{\boldsymbol{\theta}} - \boldsymbol{D}_\theta\dot{\boldsymbol{\theta}} + \boldsymbol{g}(\boldsymbol{\theta}_s) \tag{7}$$

with $\tilde{\boldsymbol{\theta}} = \boldsymbol{\theta} - \boldsymbol{\theta}_s$ is passive with respect to the variables $(\dot{\boldsymbol{\theta}}, \boldsymbol{u})$. Taking into consideration the passivity of all other subsystems, this enables the conclusion of passivity for the entire closed loop system. Actually, the controller can be shown to be equivalent to the formulation (4), with $\boldsymbol{K}_P = \boldsymbol{B}\boldsymbol{B}_\theta^{-1}\boldsymbol{K}_\theta$, $\boldsymbol{K}_D = \boldsymbol{B}\boldsymbol{B}_\theta^{-1}\boldsymbol{D}_\theta$, $\boldsymbol{K}_T = \boldsymbol{B}\boldsymbol{B}_\theta^{-1} - \boldsymbol{I}$, and $\boldsymbol{K}_S = (\boldsymbol{B}\boldsymbol{B}_\theta^{-1} - \boldsymbol{I})\boldsymbol{D}\boldsymbol{K}^{-1}$. While the structure can be effectively used for position control, it has two major drawbacks when used for impedance control. First, as mentioned before, in

order to prove the asymptotic stability, some minimal values for $\boldsymbol{K}_\theta$ (or $\boldsymbol{K}_P$) have to be ensured. This is related o the fact that the gravity compensation is done based on the desired position. For impedance control, however, the desired stiffness may be arbitrary close to zero, making gravity compensation based on desired position not meaningful. Second, the desired stiffness relation is satisfied only locally by controllers of the type give by (7), due to additional variation of the gravity term and, in the Cartesian version, of the Jacobian. In the next subsection an approach is presented, which overcomes the mentioned shortcomings. The main idea is to design the outer loop by introducing a new control variable $\bar{\boldsymbol{q}}$, which is a function of the collocated (motor) position $\boldsymbol{\theta}$ only, but is equal to the noncollocated position $\boldsymbol{q}$ (link side) in every static configuration. An iterative computation method based on the contraction mapping theorem is used to calculate this variable. A passive outer loop controller can be designed in this way, while exactly fulfilling all the steady state requirements for the system. These include not only the desired equilibrium position, but also the exact stiffness relationship between the tip position and the external force. The approach can be interpreted as a shaping of the potential energy of the robot.

3.4 The Cartesian case: Implementing exact desired stiffness

In this section, the more general case of Cartesian impedance control is treated. The joint level impedance controller can be easily derived from it. In analogy to rigid robot impedance control [13], a first choice for the outer loop controller would be:

$$\boldsymbol{u} = -\boldsymbol{J}(\boldsymbol{q})^T(\boldsymbol{K}_x\tilde{\boldsymbol{x}}(\boldsymbol{q}) + \boldsymbol{D}_x\dot{\boldsymbol{x}}(\boldsymbol{q})) + \boldsymbol{g}(\boldsymbol{q}) \ , \tag{8}$$

$$\tilde{\boldsymbol{x}}(\boldsymbol{q}) = \boldsymbol{f}(\boldsymbol{q}) - \boldsymbol{x}_s. \tag{9}$$

Herein, $\boldsymbol{x}_s$ is the desired tip configuration and $\boldsymbol{x}(\boldsymbol{q}) = \boldsymbol{f}(\boldsymbol{q})$ is the tip configuration computed by the direct kinematics map $\boldsymbol{f}$. $\boldsymbol{J}(\boldsymbol{q}) = \frac{\partial \boldsymbol{f}(\boldsymbol{q})}{\partial \boldsymbol{q}}$ is the manipulator Jacobian. $\boldsymbol{K}_x$ and $\boldsymbol{D}_x$ are positive definite matrices of desired stiffness and damping. The equilibrium conditions[2] are then given by

$$\boldsymbol{K}(\boldsymbol{\theta}_0 - \boldsymbol{q}_0) = \boldsymbol{g}(\boldsymbol{q}_0) - \boldsymbol{J}(\boldsymbol{q}_0)^T\boldsymbol{F}_{\text{ext}} \tag{10}$$

$$\boldsymbol{K}(\boldsymbol{\theta}_0 - \boldsymbol{q}_0) + \boldsymbol{J}(\boldsymbol{q}_0)^T\boldsymbol{K}_x\tilde{\boldsymbol{x}}(\boldsymbol{q}_0) = \boldsymbol{g}(\boldsymbol{q}_0), \tag{11}$$

where the relation $\boldsymbol{\tau}_{\text{ext}} = \boldsymbol{J}(\boldsymbol{q}_0)^T\boldsymbol{F}_{\text{ext}}$ between the external torque and the external tip force $\boldsymbol{F}_{\text{ext}}$ was used. Obviously, this leads to the desired stiffness relation $\boldsymbol{F}_{\text{ext}} = \boldsymbol{K}_x\tilde{\boldsymbol{x}}$ in any equilibrium position as long as $\boldsymbol{J}(\boldsymbol{q}_0)$ is invertible (what means that also $\boldsymbol{f}$ is locally invertible). The following analysis is restricted to configurations in which this assumption is fulfilled.

[2] obtained for a constant $\boldsymbol{\tau}_{\text{ext}}$ from (1),(3),(6),(8) by setting all derivatives to zero .

It is well known that the system (1) is passive with respect to the input-output pair $\{\boldsymbol{\tau}_a + \boldsymbol{\tau}_{\text{ext}}, \dot{\boldsymbol{q}}\}$. This can be shown with the storage function $S_q = \frac{1}{2}\dot{\boldsymbol{q}}^T \boldsymbol{M}(\boldsymbol{q})\dot{\boldsymbol{q}} + V_g(\boldsymbol{q})$, where $V_g(\boldsymbol{q})$ is a potential function for $\boldsymbol{g}(\boldsymbol{q})$. In order to ensure the passivity of the complete system, we are now looking for a control law for $\boldsymbol{u}$ which determines (6) to be passive in $\{\dot{\boldsymbol{q}}, -\boldsymbol{\tau}_a\}$. Obviously, (8) does not satisfy the required passivity condition. It can be observed from [19, 2, 22, 16, 5] that it is possible to ensure the passivity in $\{\dot{\boldsymbol{q}}, -\boldsymbol{\tau}_a\}$ if $\boldsymbol{u}$ is a function of $\boldsymbol{\theta}$ and its derivative only. The basic idea for the solution proposed in this paper uses the fact that, at equilibrium points, there is a one to one mapping $\boldsymbol{\theta}_0 = \boldsymbol{h}(\boldsymbol{q}_0)$ (in our case through (11)) between $\boldsymbol{\theta}_0$ and $\boldsymbol{q}_0$:

$$\boldsymbol{\theta}_0 = \boldsymbol{h}(\boldsymbol{q}_0) = \boldsymbol{q}_0 + \boldsymbol{K}^{-1}\boldsymbol{l}(\boldsymbol{q}_0), \tag{12}$$

$$\text{with}^3 \quad \boldsymbol{l}(\boldsymbol{q}_0) = -\boldsymbol{J}(\boldsymbol{q}_0)^T \boldsymbol{K}_x \tilde{\boldsymbol{x}}(\boldsymbol{q}_0) + \boldsymbol{g}(\boldsymbol{q}_0)\,. \tag{13}$$

Furthermore, the inverse mapping $\boldsymbol{h}^{-1}$ can be solved iteratively with arbitrary accuracy (see *Remark* 1).
The proposed solution consists in replacing $\boldsymbol{q}$ in (8) with $\bar{\boldsymbol{q}}(\boldsymbol{\theta}) = \boldsymbol{h}^{-1}(\boldsymbol{\theta})$ and obtaining the following controller, which is *statically equivalent* to (8):

$$\boldsymbol{u} = -\boldsymbol{J}(\bar{\boldsymbol{q}})^T(\boldsymbol{K}_x \tilde{\boldsymbol{x}}(\bar{\boldsymbol{q}}) + \boldsymbol{D}_x \boldsymbol{J}(\bar{\boldsymbol{q}})\dot{\boldsymbol{\theta}}) + \boldsymbol{g}(\bar{\boldsymbol{q}}) \tag{14}$$

$$\tilde{\boldsymbol{x}}(\bar{\boldsymbol{q}}) = \boldsymbol{f}(\bar{\boldsymbol{q}}) - \boldsymbol{x}_s. \tag{15}$$

Since $\bar{\boldsymbol{q}}(\boldsymbol{\theta}_0) = \boldsymbol{q}_0$ holds at rest, it follows that the equilibrium (10),(11) and thus the desired static relation $\boldsymbol{F}_{\text{ext}} = \boldsymbol{K}_x \tilde{\boldsymbol{x}}(\boldsymbol{q}_0)$ is still valid for this new controller. This basic idea was introduced in [16, 5] for the case of gravity compensation only and was generalized in [4] in order to provide an exact link side Cartesian stiffness. The closed loop dynamics of the system results from (1), (6), and (14):

$$\boldsymbol{M}(\boldsymbol{q})\ddot{\boldsymbol{q}} + \boldsymbol{C}(\boldsymbol{q}, \dot{\boldsymbol{q}})\dot{\boldsymbol{q}} + \boldsymbol{g}(\boldsymbol{q}) = \boldsymbol{\tau}_a + \boldsymbol{\tau}_{\text{ext}} \tag{16}$$

$$\boldsymbol{B}_\theta \ddot{\boldsymbol{\theta}} - \boldsymbol{l}(\bar{\boldsymbol{q}}) + \boldsymbol{J}(\bar{\boldsymbol{q}})^T \boldsymbol{D}_x \boldsymbol{J}(\bar{\boldsymbol{q}})\dot{\boldsymbol{\theta}} + \boldsymbol{\tau}_a = \boldsymbol{0} \tag{17}$$

Remark 1. While in general the inverse function $\bar{\boldsymbol{q}} = \boldsymbol{h}^{-1}(\boldsymbol{\theta})$ can not be computed analytically, it is possible to approximate it with arbitrary accuracy by iteration in case that the mapping $\boldsymbol{T}(\boldsymbol{q}) := \boldsymbol{\theta} - \boldsymbol{K}^{-1}\boldsymbol{l}(\boldsymbol{q})$ is a contraction. The mapping $\boldsymbol{T}(\boldsymbol{q})$ has then an unique fixed-point $\boldsymbol{q}^* = \boldsymbol{T}(\boldsymbol{q}^*) = \bar{\boldsymbol{q}}$. The iteration

$$\hat{\boldsymbol{q}}_{n+1} = \boldsymbol{T}(\hat{\boldsymbol{q}}_n) \tag{18}$$

converges thus for every starting point (e.g. $\hat{\boldsymbol{q}}_0 = \boldsymbol{\theta}$) to this fixed-point, as follows from the contraction mapping theorem (see e.g. [20]):

$$\lim_{n\to\infty} \hat{\boldsymbol{q}}_n = \boldsymbol{q}^* = \bar{\boldsymbol{q}}\ . \tag{19}$$

In order for $\boldsymbol{T}(\boldsymbol{q})$ to be a contraction, it is sufficient to show that there exists an $\alpha \in \Re$ satisfying:

[3] In [16, 5], $\boldsymbol{l}(\boldsymbol{q}_0)$ is simply $\boldsymbol{l}(\boldsymbol{q}_0) = \boldsymbol{g}(\boldsymbol{q}_0)$.

$$\left|\left|\frac{\partial \boldsymbol{l}(\boldsymbol{q})}{\partial \boldsymbol{q}}\right|\right| \leq \alpha < \frac{1}{||\boldsymbol{K}^{-1}||} \quad \forall \boldsymbol{q} \in \Re^n. \tag{20}$$

This implies the following two inequalities:

$$||\boldsymbol{l}(\boldsymbol{q}_1) - \boldsymbol{l}(\boldsymbol{q}_2)|| < \alpha||\boldsymbol{q}_1 - \boldsymbol{q}_2||, \forall \boldsymbol{q}_1, \quad \boldsymbol{q}_2 \in \Re^n \tag{21}$$

$$\begin{aligned} |V_l(\boldsymbol{q}_1) - V_l(\boldsymbol{q}_2) - (\boldsymbol{q}_1 - \boldsymbol{q}_2)^T \boldsymbol{l}(\boldsymbol{q}_2)| \\ < \alpha||\boldsymbol{q}_1 - \boldsymbol{q}_2||^2, \quad \forall \boldsymbol{q}_1, \boldsymbol{q}_2 \in \Re^n \end{aligned} \tag{22}$$

with $V_l(\boldsymbol{q})$ being a potential function for $\boldsymbol{l}(\boldsymbol{q})$. As a consequence of (21) it follows that

$$\begin{aligned} ||\boldsymbol{T}_1(\boldsymbol{q}_1) - \boldsymbol{T}_1(\boldsymbol{q}_2)|| &= ||\boldsymbol{K}^{-1}||||\boldsymbol{l}(\boldsymbol{q}_1) - \boldsymbol{l}(\boldsymbol{q}_2)|| \\ &< ||\boldsymbol{q}_1 - \boldsymbol{q}_2|| \end{aligned}$$

The condition (20) can always be fulfilled for a sufficiently small $||\boldsymbol{K}_x||$. A physical interpretation can be given as follows: ignoring gravity, the condition states that the desired Cartesian stiffness, transformed to joint space [9, 3] may not exceed the joint stiffness. On the other hand, in absence of external forces, the condition states that the joint stiffness should be high enough to sustain the robot in the gravity field. In the following it is therefore assumed that $\bar{\boldsymbol{q}}$ is known exactly. In practice, good results are obtained already by the first or second iteration step. In particular notice that by a first order approximation with $\hat{\boldsymbol{q}}_0 = \boldsymbol{q}_s$ one would obtain the second version of the controller from [22].

4 Passivity analysis

The passivity of (17) with respect to $\{\dot{\boldsymbol{q}}, -\boldsymbol{\tau}_a\}$ can be shown using the following storage function:

$$S_\theta = \frac{1}{2}\dot{\boldsymbol{\theta}}^T \boldsymbol{B}_\theta \dot{\boldsymbol{\theta}} + \frac{1}{2}(\boldsymbol{\theta} - \boldsymbol{q})^T \boldsymbol{K}(\boldsymbol{\theta} - \boldsymbol{q}) - V_{\bar{l}}(\boldsymbol{\theta}), \tag{23}$$

where $V_{\bar{l}}(\boldsymbol{\theta})$ is a potential function for $\bar{\boldsymbol{l}}(\boldsymbol{\theta}) = \boldsymbol{l}(\bar{\boldsymbol{q}}(\boldsymbol{\theta}))$. It should be mentioned that a potential function for $\boldsymbol{l}(\bar{\boldsymbol{q}}(\boldsymbol{\theta}))$ with $\boldsymbol{\theta}$ as an argument is required in (23), satisfying $\frac{\partial V_{\bar{l}}(\boldsymbol{\theta})}{\partial \boldsymbol{\theta}} = \bar{\boldsymbol{l}}(\boldsymbol{\theta})^T = \boldsymbol{l}(\bar{\boldsymbol{q}}(\boldsymbol{\theta}))^T$. A potential function $V_l(\bar{\boldsymbol{q}})$ in $\bar{\boldsymbol{q}}$, (with $\frac{\partial V_l(\bar{\boldsymbol{q}})}{\partial \bar{\boldsymbol{q}}} = \boldsymbol{l}(\bar{\boldsymbol{q}})^T$) can easily be found:

$$V_l(\bar{\boldsymbol{q}}) = -\frac{1}{2}\tilde{\boldsymbol{x}}^T(\bar{\boldsymbol{q}})\boldsymbol{K}_x\tilde{\boldsymbol{x}}(\bar{\boldsymbol{q}}) + V_g(\bar{\boldsymbol{q}})\,. \tag{24}$$

In [4] it is then shown that the required potential function $V_{\bar{l}}(\boldsymbol{\theta})$ is related to $V_l(\bar{\boldsymbol{q}})$ through

$$V_{\bar{l}}(\boldsymbol{\theta}) = V_l(\bar{\boldsymbol{q}}(\boldsymbol{\theta})) + \frac{1}{2}\boldsymbol{l}^T(\bar{\boldsymbol{q}}(\boldsymbol{\theta}))\boldsymbol{K}^{-1}\boldsymbol{l}(\bar{\boldsymbol{q}}(\boldsymbol{\theta})). \tag{25}$$

For robots with rotational joints, $-V_g(\bar{\boldsymbol{q}})$ is lower bounded. By substituting (25) and (24) into (23), it follows that S_θ is bounded from below since all other terms are positive (quadratic). Thus S_θ represents an appropriate storage function.
The time derivative of (23) along the solutions of (17) is:

$$\dot{S}_\theta = -\dot{\boldsymbol{\theta}}^T \boldsymbol{J}^T(\bar{\boldsymbol{q}}) \boldsymbol{D}_x \boldsymbol{J}(\bar{\boldsymbol{q}}) \dot{\boldsymbol{\theta}} - (\dot{\boldsymbol{\theta}} - \dot{\boldsymbol{q}})^T \boldsymbol{D} (\dot{\boldsymbol{\theta}} - \dot{\boldsymbol{q}}) - \dot{\boldsymbol{q}}^T \boldsymbol{\tau}_a .$$

The last term represents the exchanged power of the subsystem and the other terms are negative definite dissipation terms. This shows that the subsystem is indeed passive with respect to $\{\dot{\boldsymbol{q}}, -\boldsymbol{\tau}_a\}$. If the robot is contacting an environment which is also passive (with respect to $\{\dot{\boldsymbol{q}}, -\boldsymbol{\tau}_{\text{ext}}\}$), then the passivity of the entire system is given as a parallel and feedback interconnection of passive subsystems (Fig. 4).
As already mentioned before, the results of the passivity analysis have important implications for the robot interaction with the environment. Without going into details it should be mentioned that the storage functions from the passivity analysis can be used also as a Lyapunov function for the proof of asymptotic stability in the case of free motion [4].

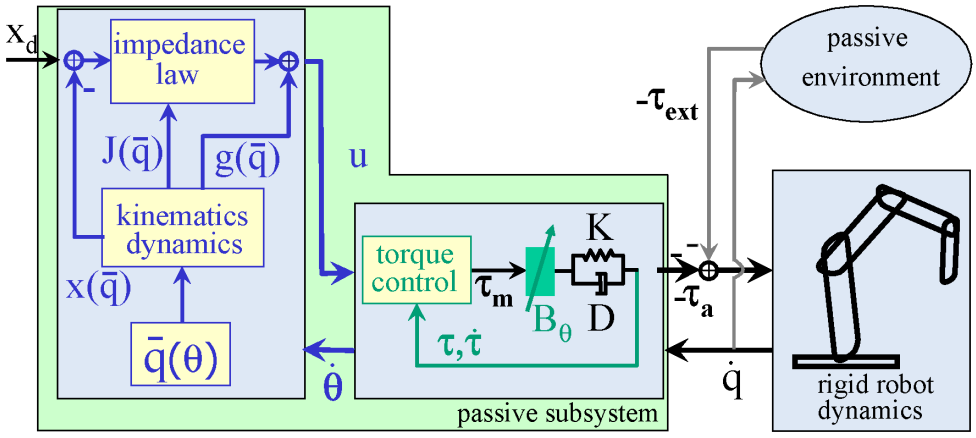

Fig. 4. Representation of the closed loop system as parallel and feedback interconnection of passive systems.

5 Experimental Evaluation

A typical impact experiment with the seven-dof DLR-light-weight-robot-II is shortly described in this section, in order to illustrate the controller perfor-

mance. For the experiment a diagonal form of the Cartesian stiffness matrix $\boldsymbol{K}_x$, with the values of Table 1, was chosen. In the experiment a desired trajec-

Table 1. Chosen values for the diagonal Cartesian stiffness matrix.

x	y	z	roll	pitch	yaw
4000 $\frac{\text{N}}{\text{m}}$	4000 $\frac{\text{N}}{\text{m}}$	4000 $\frac{\text{N}}{\text{m}}$	300 $\frac{\text{Nm}}{\text{rad}}$	300 $\frac{\text{Nm}}{\text{rad}}$	300 $\frac{\text{Nm}}{\text{rad}}$

tory $z_d(t)$ along the vertical z-axis of the end-effector frame was commanded such that the robot hit a wooden surface. During this impact, the Cartesian contact force was measured by a six-dof force-torque-sensor[4]. The measurement of the external forces was done here only for the evaluation, but is not needed for the implementation of the controller. Furthermore, the end-effector coordinate $z(\boldsymbol{q})$ was computed from the link side angles $\boldsymbol{q} = \boldsymbol{\theta} + \boldsymbol{K}^{-1}\boldsymbol{\tau}$. The resulting motion $z(\boldsymbol{q})$ and the contact force F_z of the end-effector in z-direction are shown in Fig. 5. In order to evaluate the resulting impedance relationship,

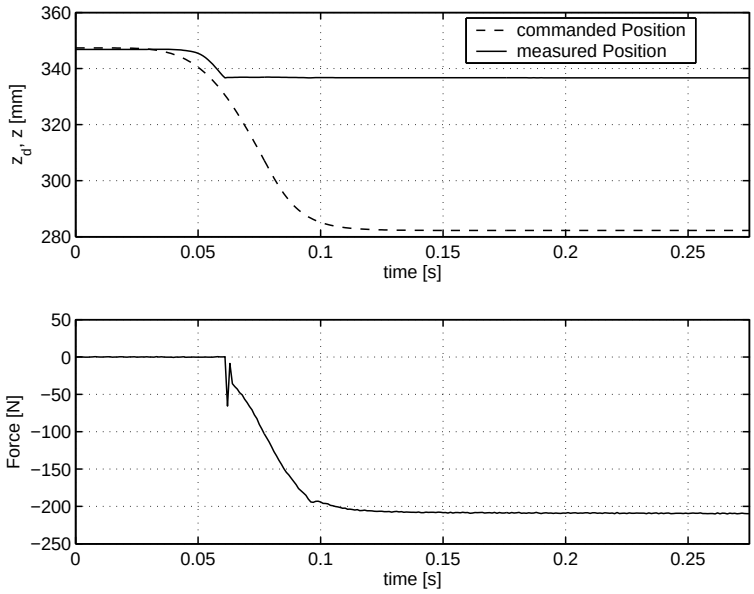

Fig. 5. The upper plot shows the desired and measured end-effector motion in z-direction during the impact experiment. In the lower plot the contact force in z-direction is displayed.

[4] A JR3-sensor was used for this.

the ratio $\frac{F_z}{z_d - z(\boldsymbol{q})}$ was computed as an estimation of the stiffness[5]. This estimation is of course only valid in the steady state. The result is shown in Fig. 6. At the steady state the estimated stiffness reaches nearly the desired value of

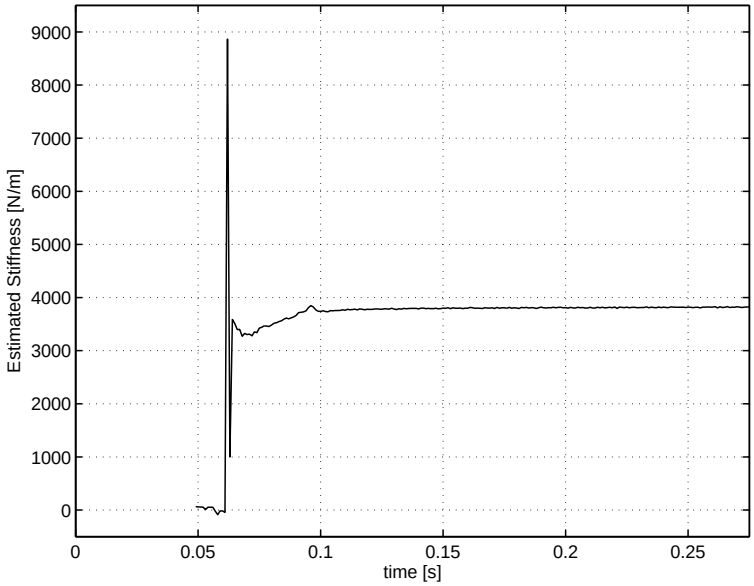

Fig. 6. Stiffness Estimation during the impact experiment.

4000N/m. The remaining difference lies in the range of known stiction effects for this robot.

6 Applications

In this section, some applications based on the presented controllers are shortly presented.

Piston insertion

Teaching by demonstration is a typical application for the impedance controller structure. A practical example was given with the task of teaching and automatic insertion of a piston into a motor block. Teaching is realized by guiding the robot with the human hand (Fig.7). It was initially known that the axes of the holes in the motor block were vertically oriented. In the teaching phase, high stiffness components for the orientations were commanded,

[5] beginning at time $0.5s$, when the robot movement started

while the translational stiffness was set to zero. This allowed only translational movements to be demonstrated by the human operator. In the second phase, the taught trajectory has been automatically reproduced by the robot. In this phase, high values were assigned for the translational stiffness, while the stiffness for the rotations was low. This enabled the robot to compensate for the remaining position errors. In this experiment, the assembly was executed automatically four times faster than by the human operator in the teaching phase. For two pistons, the total time for the assembly was 6s. The insertion task has been implemented before by using an industrial robot and a compliant force-torque sensor. Despite a well tuned Cartesian force controller, the insertion process had to be performed much slower, because of the well known control problems which occur in the case of hard contacts with conventional robots. Thus, the advantage of a compliant manipulator with stiffness control in assembly tasks became obvious.

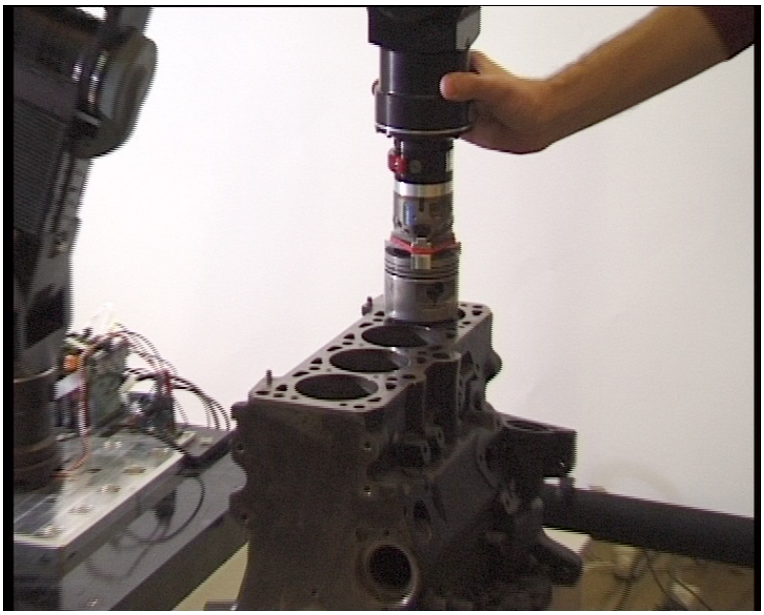

Fig. 7. Teaching phase for the automatic piston insertion using the light-weight robot II.

Wiping the table

Here the demand for a compliant behaviour of the robot also arise from reasons of safety for humans interacting with it, while the contact to the environment (table) was quite soft due to the cloth and hence not as challenging as in the

case of piston insertion. The whole task was split up into similar guiding and impedance control phases as in the piston insertion application. Fig. 8 shows a demo at the Hanover fair where the robot's elbow is deflected within its null space, while the robot continues wiping the table and applying a constant force in vertical direction.

Fig. 8. Table wiping with null space movement.

Opening a Door

In another service robotics application we used the Cartesian impedance control of the DLR light-weight robot II in order to open a door. Here the arm was used in combination with a mobile platform and the DLR-hand-II, Fig. 9.

In this application, first, the door handle was manipulated by a sequence of impedance controlled movements in order to open the door. During these motions the measurements of the joint torques provided an estimate of the contact force and thus of the current contact state.

When the mobile platform finally moved through the door hinge, the door was kept at a distance by impedance control of the arm. Therefore, instead of using the stiffness term from Section 3.4, in this stage the desired impedance was based on an appropriate potential function which has its minimum all

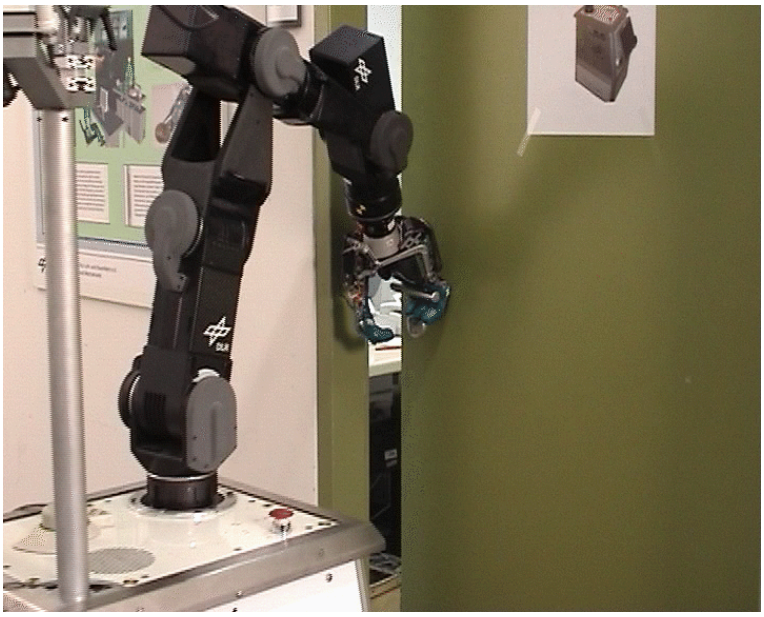

Fig. 9. DLR light-weight robot II while opening a door.

along a circularly shaped path with respect to a platform fixed frame. Additionally, the rotational stiffness was set to zero such that the end-effector orientation automatically adjusted.

7 Conclusions

In this paper, a unified, passivity based perspective was given to the problem of position, torque and impedance control of flexible joint robots, both on joint and Cartesian level. These methods are especially relevant for light-weight, compliant robots designed for service applications or for human-robot interaction. A physical interpretation was given for the torque controller and an energy shaping method was designed, which is based only on motor position (collocated controller), but which satisfies the static requirements formulated in terms of the robot tip. Without going into details, it is worth noting that the proposed energy shaping method can be generalized to a broader class of underactuated Euler-Lagrange systems [6], namely to such systems which can be stabilized by shaping of the potential energy only. An important advantage of these passivity-based controllers is the robustness with respect to uncertainties of the robot or load parameters, as well as to contact situations with unknown but passive environments. These properties were validated during numerous applications with the DLR light-weight robots.

References

1. A. Albu-Schäffer. *Regelung von Robotern mit elastischen Gelenken am Beispiel der DLR-Leichtbauarme*. PhD thesis, Technical University Munich, april 2002.
2. A. Albu-Schäffer and G. Hirzinger. A globally stable state-feedback controller for flexible joint robots. *Journal of Advanced Robotics, Special Issue: Selected Papers from IROS 2000*, 15(8):799–814, 2001.
3. A. Albu-Schäffer and G. Hirzinger. Cartesian impedance control techniques for torque controlled light-weight robots. *IEEE International Conference of Robotics and Automation*, pages 657–663, 2002.
4. A. Albu-Schäffer, C. Ott, and G. Hirzinger. Passivity based cartesian impedance control for flexible joint manipulators. *Proc. 6-th IFAC-Symposium on Nonlinear Control Systems, Stuttgart*, 2:111, 2004.
5. A. Albu-Schäffer, C. Ott, and G. Hirzinger. A passivity based cartesian impedance controller for flexible joint robots - part ii:full state feedback, impedance design and experiments. *ICRA*, pages pp. 2666–2673, 2004.
6. A. Albu-Schäffer, C. Ott, and G. Hirzinger. Constructive energy shaping based impedance control for a class of underactuated euler-lagrange systems. *ICRA*, pages 1399–1405, 2005.
7. A. Bicchi, G. Toniettiand M. Bavaro, and M. Piccigallo. Variable stiffness actuators for fast and safe motion control. *11th International Symposium of Robotics Research (ISRR)*, oct. 2003.
8. B. Brogliato, R. Ortega, and R. Lozano. Global tracking controllers for flexible-joint manipulators: a comparative study. *Automatica*, 31(7):941–956, 1995.
9. S. Chen and I. Kao. Simulation of conservative congruence transformation conservative properties in the joint and cartesian spaces. *IEEE International Conference of Robotics and Automation*, pages 1283–1288, 2000.
10. A. DeLuca. Feedforward/feedback laws for the control of flexible robots. *IEEE International Conference of Robotics and Automation*, pages 233–240, 2000.
11. A. DeLuca and P. Lucibello. A general algorithm for dynamic feedback linearization of robots with elastic joints. *IEEE International Conference of Robotics and Automation*, pages 504–510, 1998.
12. G. Hirzinger, A. Albu-Schäffer, M. Hähnle, I. Schaefer, and N. Sporer. On a new generation of torque controlled light-weight robots. *IEEE International Conference of Robotics and Automation*, pages 3356–3363, 2001.
13. N. Hogan. Impedance control: An approach to manipulation, part I - theory, part II - implementation, part III - applications. *Journ. of Dyn. Systems, Measurement and Control*, 107:1–24, 1985.
14. T. Lin and A.A. Goldenberg. Robust adaptive control of flexible joint robots with joint torque feedback. *IEEE International Conference of Robotics and Automation*, RA-3(4):1229–1234, 1995.
15. C. Ott, A. Albu-Schäffer, and G. Hirzinger. Comparison of adaptive and non-adaptive tracking control laws for a flexible joint manipulator. *IROS*, 2002.
16. C. Ott, A. Albu-Schäffer, and G. Hirzinger. A passivity based cartesian impedance controller for flexible joint robots - part i:torque feedback and gravity compensation. *ICRA*, pages pp. 2659–2665, 2004.
17. M. Spong. Modeling and control of elastic joint robots. *IEEE Journal of Robotics and Automation*, RA-3(4):291–300, 1987.
18. S. Sugano. Human-robot symbiosis. *Workshop on Human-Robot Interaction, ICRA*, 2002.

19. P. Tomei. A simple PD controller for robots with elastic joints. *IEEE Transactions on Automatic Control*, 36(10):1208–1213, 1991.
20. M. Vidyasagar. *Nonlinear Systems Analysis*. Prentice-Hall, 1978.
21. M. Zinn, O. Khatib, B. Roth, and J.K. Salisbury. A new actuation approach for human friendly robot design. *Int. Symp. on Experimental Robotics, Ischia*, 2002.
22. L. Zollo, B. Siciliano, A. De Luca, E. Guglielmelli, and P. Dario. Compliance control for a robot with elastic joints. *Proceedings of the 11th International Conference on Advanced Robotics, Coimbra, Portugal*, pages pp. 1411–1416, june 2003.